NeuroImage 189 (2019) 870–877

Contents lists available at ScienceDirect

NeuroImage

journal homepage: www.elsevier.com/locate/neuroimage

Acute stress alters the 'default' brain processing

Wei Zhang [a,b,*], Mahur M. Hashemi [a,b], Reinoud Kaldewaij [a,b], Saskia B.J. Koch [a,b], Christian Beckmann [a,c,d], Floris Klumpers [a,b,1], Karin Roelofs [a,b,1]

[a] Donders Institute, Centre for Cognitive Neuroimaging, Radboud University, Nijmegen, the Netherlands
[b] Behavioural Science Institute, Radboud University, Nijmegen, the Netherlands
[c] Department of Cognitive Neuroscience, Radboud University Medical Centre, Nijmegen, the Netherlands
[d] Oxford Centre for Functional Magnetic Resonance Imaging of the Brain (FMRIB), University of Oxford, Oxford, UK

ARTICLE INFO

Keywords:
Stress
Resting-state fMRI
Functional connectivity
Resting-state networks
RSNs
Stress vulnerability
Stress reactivity

ABSTRACT

Active adaptation to acute stress is essential for coping with daily life challenges. The stress hormone cortisol, as well as large scale re-allocations of brain resources have been implicated in this adaptation. Stress-induced shifts between large-scale brain networks, including salience (SN), central executive (CEN) and default mode networks (DMN), have however been demonstrated mainly under task-conditions. It remains unclear whether such network shifts also occur in the absence of ongoing task-demands, and most critically, whether these network shifts are predictive of individual variation in the magnitude of cortisol stress-responses.

In a sample of 335 healthy participants, we investigated stress-induced functional connectivity changes (delta-FC) of the SN, CEN and DMN, using resting-state fMRI data acquired before and after a socially evaluated cold-pressor test and a mental arithmetic task. To investigate which network changes are associated with acute stress, we evaluated the association between cortisol increase and delta-FC of each network.

Stress-induced cortisol increase was associated with increased connectivity within the SN, but with decreased coupling of DMN at both local (within network) and global (synchronization with brain regions also outside the network) levels.

These findings indicate that acute stress prompts immediate connectivity changes in large-scale resting-state networks, including the SN and DMN in the absence of explicit ongoing task-demands. Most interestingly, this brain reorganization is coupled with individuals' cortisol stress-responsiveness. These results suggest that the observed stress-induced network reorganization might function as a neural mechanism determining individual stress reactivity and, therefore, it could serve as a promising marker for future studies on stress resilience and vulnerability.

1. Introduction

Beyond traditional group-level analyses, recent investigations have moved towards characterizing individual profiles of functional connectivity (FC), which predict cognitive and behavioral performance at the single-subject level (Finn et al., 2017; Marquand et al., 2017). FC fingerprints, derived from resting-state fMRI (rs-fMRI) data in particular, have been widely used in studies examining the abnormalities of connectivity profiles in patients with stress-related psychiatric disorders (Koch et al., 2016; Nicholson et al., 2015; Oathes et al., 2015). However, it remains unclear how stress induction leads to changes in resting-state FC (rs-FC) profiles and how those changes may be linked to central stress-response systems, the major of which is the hypothalamic pituitary adrenal (HPA) axis.

Stress-related disorders like post-traumatic stress disorder (PTSD) have been suggested to be characterized by abnormal organization and functioning of three major large-scale brain networks, namely the salience network (SN), central executive network (CEN) and default model network (DMN; Menon, 2011). The interpretability of these findings however, hinges on whether they can be linked to quantitative biological markers of acute stress states such as the HPA-axis activity and its end product cortisol, which have extensively been linked to stress adaptation (De Kloet et al, 2005; McEwen, 1998). To understand the functional implications of neural network shifts in relation to stress

* Corresponding author. Kapittelweg 29, 6525 EN, Nijmegen, the Netherlands.
E-mail address: w.zhang@donders.ru.nl (W. Zhang).
[1] Equal author contributions.

https://doi.org/10.1016/j.neuroimage.2019.01.063
Received 27 June 2018; Received in revised form 16 January 2019; Accepted 24 January 2019
Available online 28 January 2019

adaptation, a number of recent investigations directly manipulated acute stress states and found that exposure to stress-induction helps reveal the fundamental neural origins of individual stress responsiveness (Cousijn et al., 2010; Henckens et al., 2012; van Oort et al., 2017). At the network level, a small number of promising studies have revealed a stress-induced re-allocation of neural resources entailing increases in SN connectivity at the cost of decreases in CEN connectivity (Hermans et al. 2011, 2014). This dynamic re-prioritization can generally be beneficial as it allows for adaptive responses to changing environmental conditions.

Importantly, these large-scale network shifts after stress induction have mainly been identified under task conditions so far (Hermans et al., 2011, 2014; McMenamin and Pessoa, 2015; Young et al., 2016). Due to the dominant roles of the SN and CEN to meet ongoing task-demands (Dosenbach et al., 2007; Seeley et al., 2007), this potentially biases the observed network shifts towards states involving SN and CEN functioning, and reduces variations in internally-driven neural fluctuations (i.e., resting-state DMN). It therefore remains unclear whether stress induction could result in similar network shifts when external task demands are absent, as in a resting-state. So far, there has been very little investigation of system-level resting-state network connectivity changes after stress induction. While limited evidence from studies using a seed-based approach suggest a general increase in the SN connectivity and mixed patterns in different DMN regions after stress induction (see review by van Oort et al., 2017), observations from clinical populations with stress-related disorders indicate the involvement of increased SN and reduced DMN connectivity in psychopathology (Admon et al., 2013; Koch et al., 2016). Accordingly, we predicted that with our network approach, we would observe similar increases in the SN connectivity and decreases in the DMN connectivity after stress induction while no changes in CEN connectivity were expected.

Most critically, despite the well-known variation in individual stress-responses, it remains unclear whether those network shifts are associated with individual stress response sensitivity, in part because most of those studies were not adequately powered to detect individual differences (van Oort et al., 2017). Until now, limited evidence has suggested that stress-induced FC increases in the SN under task conditions might be linked to individual variances in cortisol, α-amylase and subjective stress responses (Hermans et al., 2011), as well as to instant heart-rate changes (Young et al., 2016). This leaves the question open whether these observations are linked to specific task conditions or represent a shift in default functioning of these neural networks. In the current study, we aimed to test the hypothesis that acute stress-induced rs-FC changes in large-scale networks would occur as a function of individual differences in the cortisol stress-responses. Specifically, we expected stronger cortisol increases to be associated with increased SN and decreased DMN connectivity.

We tested our hypothesis in a well-powered sample of healthy individuals (N = 335), who underwent a formal stress induction, preceded and followed by rs-fMRI scans (i.e. without external stimuli input). In specific, we investigated stress-induced network connectivity changes within the SN, CEN and DMN (i.e. local connectivity changes), as well as their synchronization with other brain regions (i.e., global connectivity changes; Cole et al., 2012; Cole et al., 2011; Gonzalez-Castillo et al., 2015). By assessing both local and global connectivity changes, the current study aimed to capture a wider picture of the connectivity patterns following stress induction, not only specifically within the restricted areas (i.e., within each network) but also in the areas extending beyond our network definition. Further, to understand functional implications of these network reorganizations, we tested if these connectivity changes would occur as a function of the individual cortisol-stress reactivity.

2. Materials and methods

2.1. Participants

A total of 372 participants completed the current study. An additional group of 23 participants were tested to generate independent resting-state network templates (see details below). Exclusion criteria included any current psychiatric or neurological disorder, history of, or current endocrine or neurological treatment, current use of psychotropic medication, and current drug or alcohol abuse (full details in Koch et al., 2017). After exclusion (see more details below), data from a total of 335 participants, including 276 police students who had recently started their education at the police academy, were analysed. Sixty-one out of a total of N = 80 female participants in this sample reported hormonal contraceptive uses.

As part of a larger project consisting of multiple tests including approach-avoidance, reversal learning and emotional Go-NoGo tasks, the current study was implemented as the last experiment in the late afternoon (please refer to Koch et al., 2017 for a complete overview of the project) and was conducted in accordance with the principles of the Declaration of Helsinki and approved by the Independent Review Board Nijmegen (IRBN), the Netherlands. All participants gave their written informed consent before the study and all data were collected at the Donders Institute for Brain, Cognition and Behavior in Nijmegen, The Netherlands.

2.2. Experimental design and procedure

The experiment took place after 4PM, when cortisol levels are relatively stable because of the diurnal rhythm, so reliable individual stress-responses could be obtained (Miller et al., 2016). Two runs of fMRI scanning were implemented, one before and one after stress induction. This experiment was placed in the last imaging session of the experimental day, i.e. participants were already acquainted with the scanning procedure and thus not scanner naïve (full details of experiment protocols in Koch et al., 2017).

Stress responses were induced by sequential administration of a socially evaluated cold pressor task (SECPT) and a mental arithmetic (MA) task, a procedure that has been shown to successfully induce psychophysiological and subjective stress responses (Luo et al., 2018; Schwabe et al., 2008). Following a similar procedure as in previous studies (Luo et al., 2018; Vogel et al., 2015), participants were instructed to immerse their right foot in icy-cold (0–3 °C) water for 3 minutes. Immediately after SECPT, a 3-minute MA task was administered. Participants were instructed to count back out loud from 2053 in steps of 17 as quickly and accurately as possible. The full stress-induction procedure lasted approximately 8 min, including instructions (full details in Supplemental Methods and Materials).

2.3. Data acquisition and analysis

2.3.1. fMRI data acquisition

Each fMRI run involved one 6-minute long resting-state fMRI scan (RS1 and RS2) and one 2-minute long field-mapping scan (not used for the current analyses), leading to a total of 8 minutes per fMRI run. Participants were instructed to lie still and to stare at a small white cross at the screen center during both scanning runs, which has been suggested to increase the reliability of within-network connectivity (Birn et al., 2013). All images were collected using a 3T Siemens Magnetom Prisma^{fit} MRI scanner (Erlangen, Germany) with a 32-channel head coil. T2*-weighted EPI BOLD-fMRI images were acquired for the resting-state scans, using a multi-band 8 protocol with an interleaved slice acquisition sequence *(slice number = 64, TR = 735ms, TE = 39ms, flip angle = 52°, voxel size = 2.4×2.4×2.4 mm^3, slice gap = 0 mm, FOV = 210 mm)* that was optimized from the standard recommended scanning protocol of the Human Connectome Project (http://protocols.humanconnectome.org/HCP/3T/imaging-protocols.html). High-resolution structural images (1×1×1 mm^3) were also acquired, using a T1-weighted MP-RAGE sequence *(TR = 2300ms, TE = 3.03ms, flip angle = 8°, FOV = 256×256×192 mm^3)*.

2.3.2. Stress measurement collection

In total, five salivary samples were taken using Salivettes® collection tubes (Sarstedt, Germany) at −10, 0, +10, +20, and +30 minutes with respect to the onset time of stress induction (Fig. 1). In a group of 61 participants, the last sample (i.e., at +30 minutes) has not been obtained, resulting in a sample of N = 311 participants with complete measurements.

Together with saliva sampling, self-reported ratings of positive and negative affect (PANAS; Watson et al., 1988) were collected. Subjective ratings on negative affect were based on the sum of the scores of the 10 negative affect items for each participant. Each rating took place on a 5-point likert scale, with the sum score consequently ranging between 10 and 50. The same subsample as mentioned above (N = 311) was measured with complete measurements at all five time points (see Fig. 1).

2.3.3. Analyses on stress measures

Statistical analyses on stress measures were carried out separately on the sample of participants with complete data for all individual stress measurements (N = 311), and on the full sample (N = 372). Only the results from the sample with complete data are reported below. Results from the full sample were highly similar and can be found in Supplemental Results.

Main effects of sampling time (subsequent time points) on salivary cortisol, α-amylase levels and negative affect sum-scores were tested to index acute stress effects, using a linear mixed model with a random intercept for each individual. As salivary cortisol has been shown to be a robust and reliable measure, frequently used as a biomarker of stress responses (Bozovic et al., 2013; Hellhammer et al., 2009), cortisol level increases (the difference between time 20 minutes and baseline 0 minute) were used to investigate the association with imaging measures. To evaluate the typical gender effect on cortisol (Kudielka and Kirschbaum, 2005; Reschke-Hernández et al., 2017), as well as potential group effects (i.e., police students vs. remaining participants) in our sample, cortisol increases were compared between those groups. In short, while we observed typical gender (but not group) effects on cortisol responses (males > females), the main resulting associations between cortisol and neural responses were found to hold when taking into account gender. Full details of these supplementary analyses can be found in Supplemental Methods and Materials.

2.4. fMRI preprocessing and analysis

2.4.1. Preprocessing

Imaging data from 10% (N = 37) of the total participants were excluded from analysis due to technical issues (N = 4), motion (based on the mean value of the relative displacement; top 5% participants from each rs-fMRI scan leading to a total of 8.5%, with N = 32 from the entire sample; Pruim et al., 2015) and incidental neurological findings (N = 1), which resulted in a sample of 335 participants, including 276 police students.

To allow for T2*equilibration effects, the first five images of each resting-state scan were discarded. Analysis of fMRI data was performed with FSL5.0.9 (FMRIB, Oxford, UK). Preprocessing included motion correction by aligning all images to the first scan using rigid body transformations, spatial smoothing with a 5 mm FWHM kernel, denoising using ICA-AROMA (Pruim et al., 2015), and high-pass filtering with a cut-off of 100 Hz. The preprocessed images were then fed into a general linear model to regress out nuisance effects. Specifically, twenty-four head motion parameters (i.e., the six realignment parameters, their temporal derivatives and the quadratic terms of both the original parameters and derivatives; Caballero-Gaudes and Reynolds, 2017; Friston et al., 1996; Zu Eulenburg et al., 2012) were included in the model to minimize the motion artefacts. Additionally, each individual T1 image

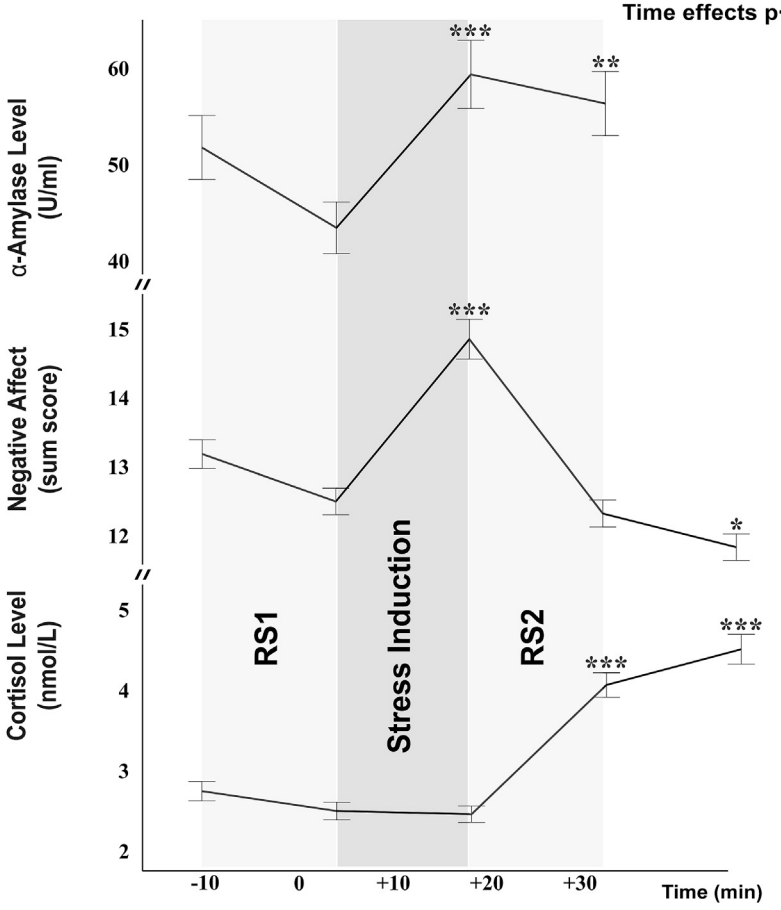

Fig. 1. Stress measures. Stress induction took place in between two runs of rs-fMRI scans (RS1 & RS2). Salivary samples and subjective affect reports were collected in a total of five times (i.e., −10m to +30m), with time interval between each sample being approximately 10 minutes. Increases in cortisol were observed 20 and 30 minutes after the onset of stress induction while increases in α-amylase and ratings of negative affect were observed immediately after stress induction (i.e., at time +10m), in comparison to baseline measurement at time 0. Of note, the last sample of α-amylase (i.e., at +30 min) was removed from the analysis due to large increases resulting from physical movement of the participants exiting the scanner room. Asterisks indicated statistically significant differences relative to time 0 immediately preceding stress induction (***p < .0001, **p < .001, *p < .05).

was segmented for subject-specific white matter and CSF masks that were subsequently thresholded with a 95% probability and registered with functional image. Mean signal intensities of white matter and CSF were extracted and included in the GLM (Caballero-Gaudes and Reynolds, 2017; Satterthwaite et al., 2013).

The residual images from this linear model were normalized to the Montreal Neurological Institute template (MNI152), using linear and nonlinear transformations via boundary based registration (BBR; Greve and Fischl, 2009), FLIRT (Jenkinson et al., 2002; Jenkinson and Smith, 2001) and FNIRT (Andersson et al., 2007). Consequently, each participant had two normalized residual images (i.e., cleaned rs-fMRI data) that index BOLD signal fluctuations, before and after acute stress induction, respectively.

2.4.2. Identifying delta-FC of RSNs

Group-level network templates based on data of 23 independently tested non-stressed participants were produced, using group independent component analysis (ICA) as implemented in MELODIC (Beckmann and Smith, 2005). ICA components showing the highest cross-correlation of mean time-series with pre-selected functional ROIs (i.e., anterior SN, left CEN, right CEN and ventral DMN) from the Stanford FIND atlas (Shirer et al., 2012) were identified as RSNs of interest. This approach allowed us to select RSNs of interest that were not biased towards the data either before or after stress induction. Importantly, the final selected RSN templates involves all major nodes/areas that are typically considered as hub regions in those networks (Fig. S1). For example, the selected SN included the bilateral anterior insula, dorsal ACC and amygdala; the CEN included dorsolateral prefrontal cortex and posterior parietal cortex while the DMN included ventromedial prefrontal cortex, parahippocampal gyrus, posterior cingulate cortex and precuneus. Connectivity changes after stress induction (i.e., delta-FC) were defined as the differences in each network of interest before and after stress induction. All individual increased (after > before) and decreased (before > after) delta-FC images were then tested at the group-level, using permutation tests via Randomise (Winkler et al., 2014), to examine significant delta-FC after stress induction for each network at both local (i.e., within network) and more global (i.e., synchronization with regions both within and outside our network definitions) levels.

The results from these initial exploratory tests were considered significant using a family-wise-error (FWE) corrected p-value of 0.00625, derived from a threshold-free cluster enhancement approach (Smith and Nichols, 2009) that accounts for the number of individual networks (i.e., SN, LCEN, RCEN, DMN), as well as the number of connectivity change directions (i.e., increases and decreases) involved in the comparisons.

2.4.3. Linking delta-FC of RSNs to stress responses

Although the lack of a non-stressful control group of adequate size precluded a direct group comparison for testing the specificity of the observed stress effects in the initial group analysis, the large sample size (N = 335) of the current study allowed us to verify that the observed connectivity changes in large-scale networks indeed covaried with individual responsiveness of the HPA axis, and therefore linked to changes in the stress response. To this end, increased cortisol level was added as a covariate in the permutation tests to link the connectivity changes to acute stress-responses. To examine significant stress-related changes within each network (i.e., local delta-FC), we used our group ICA templates (see above) as the masks for small volume correction (SVC) to directly test our a priori hypotheses. As we had no hypothesis to test the CEN unilaterally, individual delta-FC of the left and right CEN for each participant were combined for these, and all following hypothesis-testing analyses. Results from group permutation tests with cortisol increase as covariates were considered significant with a FWE corrected p-value of 0.0167 that takes into account the number of hypothesis tests for three networks (i.e., SN, CEN and DMN), using Bonferroni correction.

In addition to the standard univariate voxel-wise approach described above, we also investigated individual differences at the network level. To this end, mean coefficients of delta-FC were extracted from the clusters that showed significant connectivity changes after stress induction (Fig. S2). These coefficients indicated the strength of delta-FC between each RSN and all brain regions that showed changes in connectivity after stress induction (i.e., widespread changes referred as global synchronization including both changes with brain regions within- and outside the network), and were correlated with cortisol increase across participants. To test whether any association between delta-FC coefficients and cortisol increases existed specifically within each network (i.e., local changes), mean coefficients of individual delta-FC maps were extracted with masks of our group ICA templates. We firstly tested statistical significance of mean coefficients, using one-sample *t*-test (see results in the Supplemental Methods and Materials). Subsequently, Spearman rank correlation analyses were used to test above associations, which minimize the potential influences from extreme values in the variables. Results were considered significant with an adjusted p-value of $p < .0167$ to account for the number of analyses that were carried out to test our a priori hypotheses on three RSNs. Bootstrapped confidence intervals (boot.CI) were calculated for these rank correlation analyses, using the adjusted bootstrap percentile (BCa) method with n = 1000 iterations.

3. Results

3.1. Stress measures

Stress-induction was successful as was indicated by significant increases in all stress measures. Specifically, main effects of sampling time were observed for salivary cortisol ($F(4,1182.08) = 145.76$, $p < .0001$), α-amylase ($F(3830.97) = 9.78$, $p < .0001$) and negative affect ratings ($F(4,1230.01) = 99.24$, $p < .0001$; Fig. 1).

In line with the delayed cortisol stress responses (Schwabe et al., 2008; Kirschbaum and Hellhammer, 1994), cortisol levels significantly increased at +20 and + 30 minutes after the onset of stress induction compared to pre-stress baseline (i.e., at time 0 minute; all p's < 0.0001), while no significant difference was observed between +20 and + 30 minutes ($t(1181.93) = -2.64$, $p = .06$; Fig. 1). As expected, α-amylase and subjective stress levels peaked immediately after stress induction (i.e., at time +10 minutes; $t_{\alpha\text{-amylase}}(829.36) = -4.68$, $p < .0001$; $t_{affect}(1229.13) = -14.18$, $p<.0001$). While α-amylase level remained high (i.e., at time +20 minutes; $t(831.08) = -4.03$, $p < .001$), subjective scores of negative affect quickly declined again (i.e., at time +20 minutes; $t(1229.13) = 1.27$, $p = .71$) and eventually ended below the pre-stress baseline (i.e., time 0; $t(1229.44) = 3.74$, $p < .005$).

3.2. Cortisol-related FC changes of RSNs

Following acute stress induction, whole-brain analyses revealed both increased and decreased connectivity patterns for all four RSNs with wide-spread regions (*Supplemental Results;* Fig. S2; Table S1). To investigate the functional implications of these connectivity changes, we linked the observed delta-FC to the stress response marker cortisol. Our voxel-wise analyses identified an increased overall connectivity of the SN with a cluster in the right dACC predictive of individual cortisol increase (Bonferroni correction adjusted $p_{FWE}<.0167$; Fig. 2). Additional control tests further confirmed that this effect was not associated with head motion change, defined as the difference in the mean value of relative frame-wise displacement between RS1 and RS2 ($Rs = -0.07$, $p = .22$). No other networks showed connectivity increases or decreases related to the cortisol stress response in the voxel-wise analysis.

Thereafter, we calculated the average connectivity changes across all regions showing significant increase or decrease, separately, for each of three resting-state networks and correlated them with individual cortisol increases. At this more global level, reductions in DMN connectivity with the regions also outside the network was significantly correlated with cortisol responses ($Rs = -0.16$, Bonferroni correction adjusted $p < .0167$, boot.CI=(0.050, 0.266); Fig. 3A). Further investigation

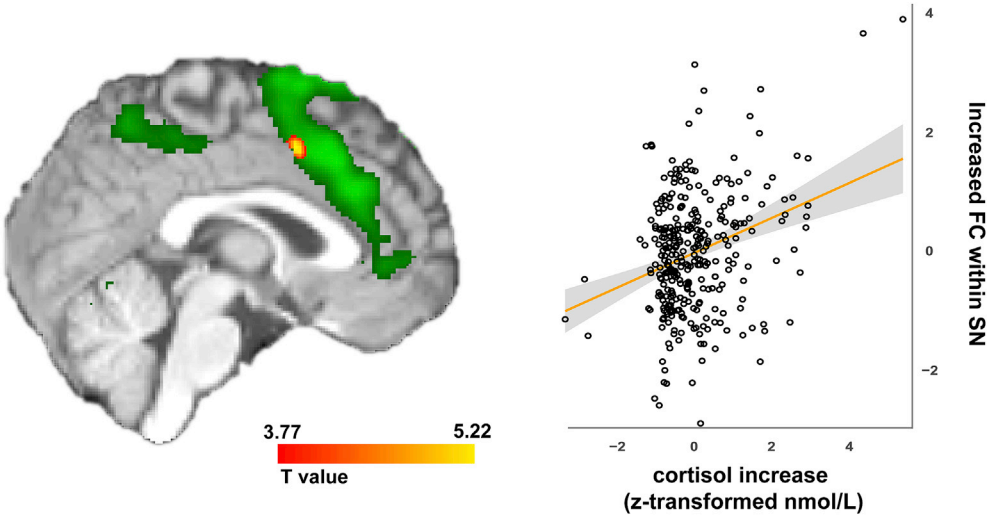

Fig. 2. Increased overall SN connectivity with dorsal ACC (red-yellow, a core SN subregion) was associated with cortisol increase in response to acute stress induction. Results shown on the left panel are whole brain corrected without additional correction for the number of networks for visualization purpose ($P_{fwe}<.05$) and imposed on our ICA-derived SN template that was used to restrict the search space (green; $z>3$). Results illustrated on the right panel are individual cortisol increase against mean coefficients extracted from individual increased SN, using the cluster showing significant increases as the mask (Bonferroni adjusted $P_{fwe}<.0167$). Follow-up tests confirmed that this effect was not driven by extreme values: the association remained significant also when the data of $N=3$ participants with relatively extreme values (i.e., >3std from the mean) were removed ($Rs=0.16$, $p<.005$).

revealed a trend of correlation between this globally decreased DMN connectivity and the head motion changes ($Rs=0.10$, $p=.06$). However, results from a multiple regression model confirmed the association between DMN connectivity decrease and cortisol increase when effects of head motion were controlled ($t(315)=2.58$, $p<.05$).

Concerning the connectivity changes within networks as a function of individual differences in cortisol responses, we found an association between the decreased delta-FC within the DMN and larger cortisol increases (FIND atlas vDMN mask, $Rs=-0.16$, Bonferroni correction adjusted $p<.0167$, boot.CI=(-0.27, −0.05); ICA-derived DMN group template, $Rs=-0.11$, $p=.047$, boot.CI=(-0.22, −0.0007); Fig. 3B). None of those RSN changes showed correlations with the head motion changes (p's > 0.11) and none of the other RSNs showed such a linkage with cortisol increase (p's > 0.05).

4. Discussion

The current study investigated rapid, stress-induced connectivity-changes *within* major resting-state networks (SN, CEN, DMN), as well as *between* these networks and other brain regions as a function of individual stress-response magnitude, measured by the stress-hormone cortisol. Specifically, cortisol stress response levels were associated with increased connectivity within SN, the network that is critical for detecting behaviorally relevant stimuli and for coordinating neural resources in response to these stimuli. Interestingly, the results also show that the reduction in local (i.e., within network) and global synchronization of DMN, known for its involvement in internal processing and homeostasis, was linked to individual differences in stress-induced cortisol levels. These findings match with the idea of a stress-induced network reorganization and suggest that increased SN and decreased DMN connectivity may function as relevant neural indicators for stress responsiveness.

In line with previous findings, we observed connectivity changes of large-scale networks following stress induction (Fig. S2; Table S1). Given our interest in RSN connectivity changes in relation to the individual stress-responses, we specifically linked the observed delta-FC to cortisol increase at the individual level. Concerning within-network delta-FC (i.e., local changes), our voxel-wise results demonstrate that cortisol-stress responses were associated with connectivity increases within the SN even when there is limited external input (i.e. during a resting-state scan). This extends previous observations of increased SN connectivity in response to acute stress induction during task-positive conditions (Hermans et al., 2011; Young et al., 2016; van Oort et al., 2017). Specifically, we identified increased connectivity between the SN as a whole and its subregion, the dACC in participants with high cortisol stress responses. As a crucial node of the SN, the dACC has been implicated in diverse functions at the intersection of cognition and emotion including interoceptive-autonomic processing (Craig, 2002; Critchley et al., 2004), pain and negative affect processing (Rotge et al., 2015) and integrating information relevant for cognitive control (Shenhav et al., 2013),

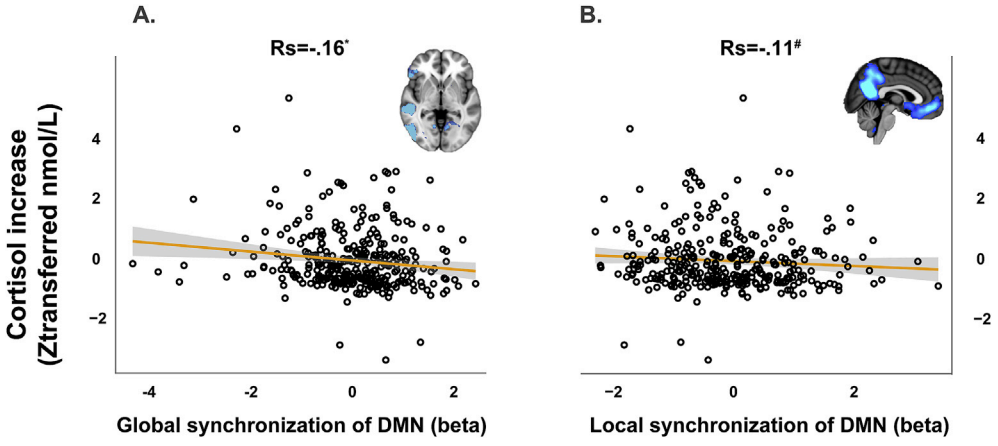

Fig. 3. Stress-induced cortisol increases are correlated with reduced synchronization at a more global level between DMN and brain regions also outside of the network, such as frontal gyrus and temporal gyrus[a] (A) and at a local level within the DMN (B). Stress-induced connectivity changes are indexed by mean coefficients at the x-axis, extracted from each participant using a connectivity map that contains all brain regions showing a significantly reduced synchronization with DMN (A), and using the ICA-derived DMN group template (B), respectively. Brain images depicted the masks that were used to extract aforementioned coefficients.
#p < .05.
*p < .0167 (Bonferroni corrected).
[a] full list can be found in Supplementary Table S1.

suggesting potential involvement of this region in responding to challenging conditions and the appraisal and expression of anxiety (Etkin et al., 2011). Abnormalities in dACC and more generally in SN connectivity have been implicated as the neurobiological correlate of enhanced salience or threat processing, a major characteristic of stress-related psychiatric disorders (Etkin and Wager, 2007; Koch et al., 2016; Vaisvaser et al., 2013).

With respect to changes in global synchronization, we found that higher cortisol increases after stress induction were associated with larger reductions in global synchronization of DMN (i.e., reductions in the interaction between the whole DMN and widespread brain regions also outside the DMN, as listed in Table S1 "decreased FC with DMN"). Interestingly, a similar association was also identified for the overall connectivity decrease within the DMN, indicated by the reduced mean coefficient of delta-FC from the FIND atlas-defined network core regions. These results suggests the involvement of the DMN in the processing of acute stress induction without on-going task demands that was not captured in the previous investigations (Young et al., 2016; Hermans et al., 2011). The DMN has largely been linked to self-referential processes (Andrews-Hanna et al., 2010; Buckner et al., 2008). Alterations in the DMN connectivity have consistently been implicated in various psychiatric disorders and particularly in stress-related disorders. For example, reduced baseline DMN connectivity has been linked to PTSD patients, while insufficient suppression of DMN has been implicated in remitted major depression (Admon et al., 2013; Bartova et al., 2015; Koch et al., 2016).

With enhanced SN connectivity on the one hand, yet reduced DMN connectivity on the other, our findings are generally in line with previous investigations that demonstrated a stress-induced network shift towards the SN (Hermans et al., 2011, 2014). In the current study, however, such a reallocation of neural resources appears to occur between the SN and DMN rather than CEN, when no external stimuli (i.e., ongoing stressors) are present. Our findings of an opposite impact of stress on connectivity of the DMN and SN appear compatible with theories of a neural resource reassignment from the DMN to the SN in the interest of processing more relevant information under a stressful state (Maron-Katz et al., 2016; Quaedflieg et al., 2015; Vaisvaser et al., 2013, 2016). Nevertheless, the current study extends the literature by showing SN and DMN fluctuations in the absence of external task demands that might be dependent on the magnitude of the individual cortisol stress responses. Similar alterations in the SN and DMN connectivity have been implicated in a wide range of psychiatric disorders and particularly in stress-related disorders (Admon et al., 2013; Bartova et al., 2015; Etkin and Wager, 2007; Koch et al., 2016; Sripada et al., 2012; Vaisvaser et al., 2013). On the other hand, however, studies in animals as well as in human suggest that the HPA-axis is highly relevant for fast adaptation to stressful situations (De Kloet et al., 2005; Joëls and Baram, 2009). It will be of interest for future investigations to examine longitudinally whether the increased SN connectivity and decreased DMN connectivity indicate individual adaptation or vulnerability to acute stress induction, and whether those stress-induced neural network responses can predict the development of psychopathology after trauma exposure.

Several limitations of the present study should be mentioned. Firstly, although we recruited an independent group to derive the group network templates for imaging analysis in a non-biased fashion, it was of an insufficient sample size (N = 23) to serve as a direct control group for validating stress-induced neural effects observed in a sample of N = 335. It is possible that the lack of such a control group could potentially confound the observed stress effects at neural level with scanning order. However, this concern is mitigated by the fact that our participants were not scanner-naïve (i.e., had previously been tested in the same scanner twice on the same testing day) and showed no cortisol increases before the RS1 and stress induction. Most importantly, within our experimental group, we confirmed that both enhanced SN connectivity and reduced DMN connectivity correlated significantly with individual cortisol responsiveness. These results together strongly suggest that the observed neural effects are stress related. Secondly, the current acquisition length of 6.5 minutes is shorter than the recommended acquisition length (i.e., 9–12 min) of resting-state imaging data (Birn et al., 2013). However, together with our large sample size, the fast multi-band imaging protocol (TR = 735ms) enabled us to obtain a relatively large number of scans (N = 500) in each session, which increases the reliability of our results. Thirdly, the effect size of the observed correlations could be arguably considered small by traditional standards (i.e., coefficient between 0.1 and 0.15). Recent meta-analyses however show that traditional guidelines for interpreting correlation coefficients may have been too stringent (Gignac and Szodorai, 2016; Hemphill, 2003) because observed correlations are practically dampened by the imperfect measurement reliability of two variables in the correlation almost in any studies (Hedge et al., 2017; Vul et al., 2009). In the current study, it is very well conceivable that factors beyond our experimental control (e.g. sleep quality before the experiment day) might have influenced both the cortisol and neural responses, and thus diluted correlation effect sizes. Furthermore, evidence from simulations show that increasing sample size is generally associated with decreasing correlation coefficients and that a large sample size (e.g., N > 250) entails more stable effect size (Schönbrodt and Perugini, 2013). The small effect size of the correlations resulting from our large sample size therefore likely reflected a meaningful and robust underlying association between neural network processing and stress responses. Fourthly, it could be considered as a limitation that physiological recordings (e.g., respiration) were not included to further clean up the imaging data. However, acute stress induction has been shown to influence physiological responses. Regressing out physiological parameters further will enhance the risk of only investigating the neural processes that are independent of stress-induced sympathetic and parasympathetic activities (Murphy et al., 2013). To control for potential non-neural physiology, we followed the common practice in the literature to remove the mean intensity of the WM and CSF from the imaging data (Henckens et al., 2012; Hermans et al., 2011; Maron-Katz et al., 2016; Vaisvaser et al., 2013, 2016). More importantly, we went above and beyond this common practice by acquiring imaging data with a fast sampling sequence (i.e., multiband 8), which in combination of ICA has been shown to facilitate the identification and elimination of physiological components (Boubela et al., 2014; Parkes et al., 2018; Pruim et al., 2015). Finally, it is worth mentioning that our current resting-state connectivity measurement in the immediate aftermath of a stressor likely contains a mixture of both acute stress reactions and stress recovery processes. For future studies, including scans during stress recovery (i.e. after acute stress subsides) would be of interest in order to more systematically study the temporal dynamics of the stress-induced network changes observed here (Hermans et al., 2014; Vaisvaser et al., 2013).

In conclusion, our results demonstrate distributed connectivity changes in large-scale RSNs after stress induction. More importantly, the strengthened coupling within the SN, as well as the degree of decoupling within the DMN, and between the DMN and other brain regions, was associated with individual cortisol stress-responsiveness. These results suggest that acute stress induction alters default brain processing and that such an alteration might potentially function as a neural mechanism determining individual stress reactivity.

Acknowledgments

FK and KR contributed equally to this article. We are especially thankful to Dutch Police Academy (Politieacademie) for their cooperation and to Annika Smit for her valuable help with recruiting participants and facilitating our study. We also thank our former and current colleagues Vanessa van Ast, Ingrid Kersten, Naomi de Valk, Geoffrey Bertou, Leonore Bovy, Iris Hulzink, Tiele Dopp, Marijolein Hartgerink, Bart Becker, Madine Zoet, Delphin van Benthem, Job de Brouwer, Lisanne Nuijen, Pepijn van Houten, Klaas van Groesen and Nienke Flipsen for their help in setting up the study, recruiting participants and acquiring

data, to Maarten Mennes for his valuable suggestions to control motion artefacts, to Zahra Fazal for sharing her thoughts on physiological confounds, and to Paul Gaalman for his technical assistance in fMRI data acquisition.

Appendix A. Supplementary data

Supplementary data to this article can be found online at https://doi.org/10.1016/j.neuroimage.2019.01.063.

Funding and disclosure

This work was supported by a VICI grant (#453-12-001) from the Netherlands Organization for Scientific Research (NWO) and a starting grant from the European Research Council (ERC_StG2012_313749) awarded to Karin Roelofs. The authors report no biomedical financial interests or potential conflicts of interest.

References

Admon, R., Milad, M.R., Hendler, T., 2013. A causal model of post-traumatic stress disorder: Disentangling predisposed from acquired neural abnormalities. Trends Cognit. Sci. 17 (7), 337–347. https://doi.org/10.1016/j.tics.2013.05.005.

Andersson, J.L.R., Jenkinson, M., Smith, S., 2007. Non-linear registration, aka spatial normalisation. FMRIB Technial Report TR07JA2. Oxford Centre for Functional Magnetic Resonance Imaging of the Brain, Department of Clinical Neurology. Oxford University, Oxford, UK.

Andrews-Hanna, J.R., Reidler, J.S., Sepulcre, J., Poulin, R., Buckner, R.L., 2010. Functional-anatomic fractionation of the brain's default network. Neuron 65 (4), 550–562. https://doi.org/10.1016/j.neuron.2010.02.005.

Bartova, L., Meyer, B.M., Diers, K., Rabl, U., Scharinger, C., Popovic, A., et al., 2015. Reduced default mode network suppression during a working memory task in remitted major depression. J. Psychiatr. Res. 64, 9–18. https://doi.org/10.1016/j.jpsychires.2015.02.025.

Beckmann, C.F., Smith, S.M., 2005. Tensorial extensions of independent component analysis for multisubject FMRI analysis. Neuroimage 25 (1), 294–311. https://doi.org/10.1016/j.neuroimage.2004.10.043.

Birn, R.M., Molloy, E.K., Patriat, R., Parker, T., Meier, T.B., Kirk, G.R., et al., 2013. The effect of scan length on the reliability of resting-state fMRI connectivity estimates. Neuroimage 83, 550–558. https://doi.org/10.1016/j.neuroimage.2013.05.099.

Boubela, R.N., Kalcher, K., Nasel, C., Moser, E., 2014. Scanning fast and slow: current limitations of 3 Tesla functional MRI and future potential. Front. Phys. 2. https://doi.org/10.3389/fphy.2014.00001.

Bozovic, D., Racic, M., Ivkovic, N., 2013. Salivary Cortisol Levels as a Biological Marker of Stress Reaction. Med. Arch. 67, 374. https://doi.org/10.5455/medarh.2013.67.374-377.

Buckner, R.L., Andrews-Hanna, J.R., Schacter, D.L., 2008. The brain's default network: Anatomy, function, and relevance to disease. Ann. N. Y. Acad. Sci. 1124, 1–38. https://doi.org/10.1196/annals.1440.011.

Caballero-Gaudes, C., Reynolds, R.C., 2017. Methods for cleaning the BOLD fMRI signal. Neuroimage 154, 128–149. https://doi.org/10.1016/j.neuroimage.2016.12.018.

Cole, M.W., Anticevic, A., Repovs, G., Barch, D., 2011. Variable global dysconnectivity and individual differences in schizophrenia. Biol. Psychiatry 70 (1), 43–50. https://doi.org/10.1016/j.biopsych.2011.02.010.

Cole, M.W., Yarkoni, T., Repovs, G., Anticevic, A., Braver, T.S., 2012. Global connectivity of prefrontal cortex predicts cognitive control and intelligence. J. Neurosci. 32 (26), 8988–8999. https://doi.org/10.1523/JNEUROSCI.0536-12.2012.

Cousijn, H., Rijpkema, M., Qin, S., van Marle, H.J.F., Franke, B., Hermans, E.J., et al., 2010. Acute stress modulates genotype effects on amygdala processing in humans. Proc. Natl. Acad. Sci. Unit. States Am. 107 (21), 9867–9872. https://doi.org/10.1073/pnas.1003514107.

Craig, a. D., 2002. How do you feel? Interoception: the sense of the physiological condition of the body. Nat. Rev. Neurosci. 3 (8), 655–666. https://doi.org/10.1038/nrn894.

Critchley, H.D., Wiens, S., Rotshtein, P., Öhman, A., Dolan, R.J., 2004. Neural systems supporting interoceptive awareness. Nat. Neurosci. 7 (2), 189–195. https://doi.org/10.1038/nn1176.

De Kloet, E.R., Joëls, M., Holsboer, F., 2005. Stress and the brain: From adaptation to disease. Nat. Rev. Neurosci. 6, 463–475. https://doi.org/10.1038/nrn1683.

Dosenbach, N.U.F., Fair, D.A., Miezin, F.M., Cohen, A.L., Wenger, K.K., Dosenbach, R.A.T., et al., 2007. Distinct brain networks for adaptive and stable task control in humans. Proc. Natl. Acad. Sci. Unit. States Am. 104 (26), 11073–11078. https://doi.org/10.1073/pnas.0704320104.

Etkin, A., Egner, T., Kalisch, R., 2011. Emotional processing in anterior cingulate and medial prefrontal cortex. Trends Cognit. Sci. 15, 85–93. https://doi.org/10.1016/j.tics.2010.11.004.

Etkin, A., Wager, T.D., 2007. Functional neuroimaging of anxiety: a meta-analysis of emotional processing in PTSD, social anxiety disorder, and specific phobia. Am. J. Psychiatry 164 (10), 1476–1488. https://doi.org/10.1176/appi.ajp.2007.07030504.

Finn, E.S., Scheinost, D., Finn, D.M., Shen, X., Papademetris, X., Constable, R.T., 2017. Can brain state be manipulated to emphasize individual differences in functional connectivity? Neuroimage 160, 140–151. https://doi.org/10.1016/j.neuroimage.2017.03.064.

Friston, K.J., Williams, S., Howard, R., Frackowiak, R.S.J., Turner, R., 1996. Movement-Related effects in fMRI time-series. Magn. Reson. Med. 35 (3), 346–355. https://doi.org/10.1002/mrm.1910350312.

Gignac, G.E., Szodorai, E.T., 2016. Effect size guidelines for individual differences researchers. Pers. Indiv. Differ. 102, 74–78. https://doi.org/10.1016/j.paid.2016.06.069.

Gonzalez-Castillo, J., Hoy, C.W., Handwerker, D.A., Robinson, M.E., Buchanan, L.C., Saad, Z.S., Bandettini, P.A., 2015. Tracking ongoing cognition in individuals using brief, whole-brain functional connectivity patterns. Proc. Natl. Acad. Sci. Unit. States Am. 112 (28), 8762–8767. https://doi.org/10.1073/pnas.1501242112.

Greve, D.N., Fischl, B., 2009. Accurate and robust brain image alignment using boundary-based registration. Neuroimage 48 (1), 63–72. https://doi.org/10.1016/j.neuroimage.2009.06.060.

Hedge, C., Powell, G., Sumner, P., 2017. The reliability paradox: Why robust cognitive tasks do not produce reliable individual differences. Behav. Res. Methods 1–21. https://doi.org/10.3758/s13428-017-0935-1.

Hellhammer, D.H., Wüst, S., Kudielka, B.M., 2009. Salivary cortisol as a biomarker in stress research. Psychoneuroendocrinology 34 (2), 163–171. https://doi.org/10.1016/j.psyneuen.2008.10.026.

Hemphill, J.F., 2003. Interpreting the Magnitudes of Correlation Coefficients. Am. Psychol. 58, 78–79. https://doi.org/10.1037/0003-066X.58.1.78.

Henckens, M. J. a G., van Wingen, G. a, Joëls, M., Fernández, G., 2012. Corticosteroid induced decoupling of the amygdala in men. Cerebr. Cortex 22 (10), 2336–2345. New York, N.Y. : 1991. https://doi.org/10.1093/cercor/bhr313.

Hermans, E.J., Henckens, M.J.A.G., Joëls, M., Fernández, G., 2014. Dynamic adaptation of large-scale brain networks in response to acute stressors. Trends Neurosci. 37 (6), 304–314. https://doi.org/10.1016/j.tins.2014.03.006.

Hermans, E.J., van Marle, H.J.F., Ossewaarde, L., Henckens, M. J. a. G., Qin, S., van Kesteren, M.T.R., et al., 2011. Stress-related noradrenergic activity prompts large-scale neural network reconfiguration. Science 334 (6059), 1151–1153. https://doi.org/10.1126/science.1209603.

Jenkinson, M., Bannister, P., Brady, M., Smith, S., 2002. Improved optimization for the robust and accurate linear registration and motion correction of brain images. Neuroimage 17 (2), 825–841. https://doi.org/10.1016/S1053-8119(02)91132-8.

Jenkinson, M., Smith, S., 2001. A global optimisation method for robust affine registration of brain images. Med. Image Anal. 5 (2), 143–156. https://doi.org/10.1016/S1361-8415(01)00036-6.

Joëls, M., Baram, T.Z., 2009. The neuro-symphony of stress. Nat. Rev. Neurosci. 10 (6), 459–466. https://doi.org/10.1038/nrn2632.

Kirschbaum, C., Hellhammer, D.H., 1994. Salivary cortisol in psychoneuroendocrine research: recent developments and applications. Psychoneuroendocrinology 19 (4), 313–333. https://doi.org/10.1016/0306-4530(94)90013-2.

Koch, S.B.J., Klumpers, F., Zhang, W., Hashemi, M.M., Kaldewaij, R., van Ast, V.A., et al., 2017. The role of automatic defensive responses in the development of posttraumatic stress symptoms in police recruits: protocol of a prospective study. Eur. J. Psychotraumatol. 8 (1), 1412226. https://doi.org/10.1080/20008198.2017.1412226.

Koch, S.B.J., van Zuiden, M., Nawijn, L., Frijling, J.L., Veltman, D.J., Olff, M., 2016. Aberrant resting-state brain activity in posttraumatic stress disorder: A meta-analysis and systematic review. Depress. Anxiety 33 (7), 592–605. https://doi.org/10.1002/da.22478.

Kudielka, B., Kirschbaum, C., 2005. Sex differences in HPA axis responses to stress: a review. Biol. Psychol. 69, 113–132. https://doi.org/10.1016/j.biopsycho.2004.11.009.

Luo, Y., Fernández, G., Hermans, E., Vogel, S., Zhang, Y., Li, H., Klumpers, F., 2018. How acute stress may enhance subsequent memory for threat stimuli outside the focus of attention: DLPFC-amygdala decoupling. Neuroimage 171, 311–322. https://doi.org/10.1016/j.neuroimage.2018.01.010.

Maron-Katz, A., Vaisvaser, S., Lin, T., Hendler, T., Shamir, R., 2016. A large-scale perspective on stress-induced alterations in resting-state networks. Sci. Rep. 6 (February), 21503. https://doi.org/10.1038/srep21503.

Marquand, A.F., Haak, K.V., Beckmann, C.F., 2017. Functional corticostriatal connection topographies predict goal-directed behaviour in humans. Nat. Human Behav. 1 (8). https://doi.org/10.1038/s41562-017-0146.

McEwen, B.S., 1998. Stress, adaptation, and disease: allostasis and allostatic load. Ann. N. Y. Acad. Sci. 840 (1), 33–44. https://doi.org/10.1111/j.1749-6632.1998.tb09546.x.

McMenamin, B.W., Pessoa, L., 2015. Discovering networks altered by potential threat ("anxiety") using quadratic discriminant analysis. Neuroimage 116, 1–9. https://doi.org/10.1016/j.neuroimage.2015.05.002.

Menon, V., 2011. Large-scale brain networks and psychopathology: A unifying triple network model. Trends Cognit. Sci. 15 (10), 483–506. https://doi.org/10.1016/j.tics.2011.08.003.

Miller, R., Stalder, T., Jarczok, M., Almeida, D.M., Badrick, E., Bartels, M., et al., 2016. The CIRCORT database: Reference ranges and seasonal changes in diurnal salivary cortisol derived from a meta-dataset comprised of 15 field studies. Psychoneuroendocrinology 73 (8), 16–23. https://doi.org/10.1016/j.psyneuen.2016.07.201.

Murphy, K., Birn, R.M., Bandettini, P.A., 2013. Resting-state fMRI confounds and cleanup. Neuroimage 80, 349–359. https://doi.org/10.1016/j.neuroimage.2013.04.001.

Nicholson, A.A., Densmore, M., Frewen, P.A., Théberge, J., Neufeld, R.W.J., McKinnon, M.C., Lanius, R.A., 2015. The dissociative subtype of posttraumatic stress disorder: unique resting-state functional connectivity of Basolateral and

Centromedial Amygdala complexes. Neuropsychopharmacology 40 (10), 2317–2326. https://doi.org/10.1038/npp.2015.79.
Oathes, D.J., Patenaude, B., Schatzberg, A.F., Etkin, A., 2015. Neurobiological signatures of anxiety and depression in resting-state functional magnetic resonance imaging. Biol. Psychiatry 77 (4), 385–393. https://doi.org/10.1016/j.biopsych.2014.08.006.
Parkes, L., Fulcher, B., Yücel, M., Fornito, A., 2018. NeuroImage An evaluation of the ef fi cacy , reliability , and sensitivity of motion correction strategies for resting-state functional MRI. Neuroimage 171, 415–436. July 2017. https://doi.org/10.1016/j.neuroimage.2017.12.073.
Pruim, R.H.R., Mennes, M., van Rooij, D., Llera, A., Buitelaar, J.K., Beckmann, C.F., 2015. ICA-AROMA: A robust ICA-based strategy for removing motion artifacts from fMRI data. Neuroimage 112, 267–277. https://doi.org/10.1016/j.neuroimage.2015.02.064.
Quaedflieg, C.W.E.M., van de Ven, V., Meyer, T., Siep, N., Merckelbach, H., Smeets, T., 2015. Temporal dynamics of stress-induced alternations of intrinsic amygdala connectivity and neuroendocrine levels. PLoS One 10 (5) e0124141. https://doi.org/10.1371/journal.pone.0124141.
Reschke-Hernández, A.E., Okerstrom, K.L., Bowles Edwards, A., Tranel, D., 2017. Sex and stress: Men and women show different cortisol responses to psychological stress induced by the Trier social stress test and the Iowa singing social stress test. J. Neurosci. Res. 95 (1–2), 106–114. https://doi.org/10.1002/jnr.23851.
Rotge, J.Y., Lemogne, C., Hinfray, S., Huguet, P., Grynszpan, O., Tartour, E., et al., 2015. A meta-analysis of the anterior cingulate contribution to social pain. Soc. Cognit. Affect Neurosci. 10 (1), 19–27. https://doi.org/10.1093/scan/nsu110.
Satterthwaite, T.D., Elliott, M.A., Gerraty, R.T., Ruparel, K., Loughead, J., Calkins, M.E., et al., 2013. An improved framework for confound regression and filtering for control of motion artifact in the preprocessing of resting-state functional connectivity data. Neuroimage 64 (1), 240–256. https://doi.org/10.1016/j.neuroimage.2012.08.052.
Schönbrodt, F.D., Perugini, M., 2013. At what sample size do correlations stabilize? J. Res. Pers. 47 (5), 609–612. https://doi.org/10.1016/j.jrp.2013.05.009.
Schwabe, L., Haddad, L., Schachinger, H., 2008. HPA axis activation by a socially evaluated cold-pressor test. Psychoneuroendocrinology 33 (6), 890–895. https://doi.org/10.1016/j.psyneuen.2008.03.001.
Seeley, W.W., Menon, V., Schatzberg, A.F., Keller, J., Glover, G.H., Kenna, H., et al., 2007. Dissociable intrinsic connectivity networks for salience processing and executive control. J. Neurosci. 27 (9), 2349–2356. https://doi.org/10.1523/JNEUROSCI.5587-06.2007.
Shenhav, A., Botvinick, M.M., Cohen, J.D., 2013. The expected value of control: An integrative theory of anterior cingulate cortex function. Neuron 79, 217–240. https://doi.org/10.1016/j.neuron.2013.07.007.
Shirer, W.R., Ryali, S., Rykhlevskaia, E., Menon, V., Greicius, M.D., 2012. Decoding subject-driven cognitive states with whole-brain connectivity patterns. Cerebr. Cortex 22 (1), 158–165. https://doi.org/10.1093/cercor/bhr099.
Smith, S.M., Nichols, T.E., 2009. Threshold-free cluster enhancement: Addressing problems of smoothing, threshold dependence and localisation in cluster inference. Neuroimage 44 (1), 83–98. https://doi.org/10.1016/j.neuroimage.2008.03.061.
Sripada, R.K., King, A.P., Welsh, R.C., Garfinkel, S.N., Wang, X., Sripada, C.S., Liberzon, I., 2012. Neural dysregulation in posttraumatic stress disorder: evidence for disrupted equilibrium between salience and default mode brain networks. Psychosom. Med. 74 (9), 904–911. https://doi.org/10.1097/PSY.0b013e318273bf33.
Vaisvaser, S., Lin, T., Admon, R., Podlipsky, I., Greenman, Y., Stern, N., et al., 2013. Neural traces of stress: cortisol related sustained enhancement of amygdala-hippocampal functional connectivity. Front. Hum. Neurosci. 7, 313. https://doi.org/10.3389/fnhum.2013.00313.
Vaisvaser, S., Modai, S., Farberov, L., Lin, T., Sharon, H., Gilam, A., et al., 2016. Neuro-epigenetic indications of acute stress response in humans: The case of microRNA-29c. PLoS One 11 (1), 1–17. https://doi.org/10.1371/journal.pone.0146236.
van Oort, J., Tendolkar, I., Hermans, E.J., Mulders, P.C., Beckmann, C.F., Schene, A.H., et al., 2017. How the brain connects in response to acute stress: A review at the human brain systems level. Neurosci. Biobehav. Rev. 83 (April), 281–297. https://doi.org/10.1016/j.neubiorev.2017.10.015.
Vogel, S., Klumpers, F., Krugers, H.J., Fang, Z., Oplaat, K.T., Oitzl, M.S., et al., 2015. Blocking the mineralocorticoid receptor in humans prevents the stress-induced enhancement of centromedial amygdala connectivity with the Dorsal Striatum. Neuropsychopharmacology 40 (4), 947–956. https://doi.org/10.1038/npp.2014.271.
Vul, E., Harris, C., Winkielman, P., Pashler, H., 2009. Puzzlingly High Correlations in fMRI Studies of Emotion, Personality, and Social Cognition1. Perspect. Psychol. Sci. 4 (3), 274–290. https://doi.org/10.1111/j.1745-6924.2009.01125.x.
Watson, D., Clark, L. a., Tellegan, a., 1988. Worksheet 3.1 the positive and negative affect schedule (PANAS; Watson et al., 1988) PANAS questionnaire. J. Pers. Soc. Psychol. 54, 1063–1070. https://doi.org/10.1521/soco_2012_1006.
Winkler, A.M., Ridgway, G.R., Webster, M.A., Smith, S.M., Nichols, T.E., 2014. Permutation inference for the general linear model. Neuroimage 92, 381–397. https://doi.org/10.1016/j.neuroimage.2014.01.060.
Young, C.B., Raz, G., Everaerd, D., Beckmann, C.F., Tendolkar, I., Hendler, T., et al., 2016. Dynamic shifts in large-scale brain network balance as a function of arousal. J. Neurosci. 37, 281–290. https://doi.org/10.1523/JNEUROSCI.1759-16.2016.
Zu Eulenburg, P., Caspers, S., Roski, C., Eickhoff, S.B., 2012. Meta-analytical definition and functional connectivity of the human vestibular cortex. Neuroimage 60 (1), 162–169. https://doi.org/10.1016/j.neuroimage.2011.12.032.